Solvation Dynamics in Bile Salt Aggregates

ARTICLE *in* THE JOURNAL OF PHYSICAL CHEMISTRY B · JULY 2002

Impact Factor: 3.3 · DOI: 10.1021/jp0144799

4 AUTHORS:

Sobhan Sen
Jawaharlal Nehru University
36 PUBLICATIONS **996** CITATIONS
SEE PROFILE

Partha Dutta
M. M. C. College, University of Calcutta
21 PUBLICATIONS **485** CITATIONS
SEE PROFILE

Saptarshi Mukherjee
Indian Institute of Science Education and Re…
49 PUBLICATIONS **637** CITATIONS
SEE PROFILE

Kankan Bhattacharyya
Indian Association for the Cultivation of Scie…
231 PUBLICATIONS **7,582** CITATIONS
SEE PROFILE

ARTICLES

Solvation Dynamics in Bile Salt Aggregates

Sobhan Sen, Partha Dutta, Saptarshi Mukherjee, and Kankan Bhattacharyya*

Physical Chemistry Department, Indian Association for the Cultivation of Science, Jadavpur, Kolkata 700 032, India

Received: December 10, 2001; In Final Form: June 2, 2002

The solvation dynamics inside an aggregate of a bile salt, sodium deoxycholate (NaDC), in aqueous solution has been studied using picosecond time-resolved emission spectroscopy and two fluorescent probes, 4-(dicyanomethylene)-2-methyl-(*p*-dimethylaminostyryl)-4*H*-pyran (DCM) and 2,6-*p*-toluidinonaphthalenesulfonate (TNS). Addition of NaDC to an aqueous solution causes a nearly 110-fold increase in the emission quantum yield (ϕ_f) of TNS. From the variation of ϕ_f of TNS, two critical micellar concentrations of NaDC have been detected at around 7 and 60 mM, respectively. The solvation dynamics of TNS in 100 mM NaDC solution is described by three components, 95 ps (17%), 380 ps (16%), and 1.9 ns (67%). The solvation dynamics of DCM bound to 100 mM NaDC is also found to be triexponential with components of 110 ps (19%), 700 ps (17%), and 2.75 ns (64%). The substantially slow solvation dynamics of water in the vicinity of NaDC indicates restricted solvation dynamics of water inside the bile salt aggregate.

1. Introduction

Water molecules confined in nanocavities control the structure, dynamics, and reactivity of biological systems in a unique way.[1,2] Recently it has been demonstrated that water molecules confined in a nanocavity are markedly slower than those in bulk water. Fleming et al. reported that water molecules confined in a cyclodextrin cavity display a component of solvation dynamics which is slower than that of bulk water by 2−3 orders of magnitude.[3] Since then, such slow components have been reported for water molecules in proteins,[4,5] DNA,[6] microemulsions,[7] micelles,[8] lipid vesicles,[9] and sol−gel matrixes,[10] while solvation dynamics at the water surface is quite fast.[11] It is observed that the unusual slow dynamics is not special to water alone. Nonaqueous solvents (e.g., dimethylformamide, acetonitrile, or methanol) show ultraslow dynamics in microemusions[12] and inside a cyclodextrin cavity.[13] Several theoretical models have been proposed to explain the slow component of solvation dynamics. Most recently, simulations of solvation dynamics at different interfaces revealed the presence of such slow components.[14] In the present work, we investigate solvation dynamics in another organized medium, namely, an aggregate of a bile salt, sodium deoxycholate (NaDC).

Bile salts are naturally occurring, amphiphilic compounds which are synthesized in the liver and stored in the gallbladder.[15] Ordinary surfactants containing an alkyl chain pack into a nearly spherical micelle with a water-filled spherical shell (called a Stern layer for ionic micelles and Palisade layer for neutral ones) and a "dry" hydrocarbon core.[16] A fluorescent probe, trapped in the Stern or Palisade layer of a micelle, is almost fully shielded from bulk water. Bile salts do not possess the polar headgroups and the nonpolar aliphatic tail like ordinary surfactants. The bile salt NaDC (Chart 1) consists of a hydrophobic steroid ring and a hydrophilic portion comprising the hydroxyl groups and the ions (carboxylate anion and sodium cation). The steroid ring of a bile salt is not planar. There is a concave hydrophilic surface on one side and a convex hydrophobic surface on the other side of the steroid moiety. Micellization of bile salts and their interaction with biological membranes play an important role in billiary secretion and cholesterol solubilization.[15,16] In a slightly alkaline medium (pH > 7.5), NaDC

CHART 1: (a) Structure of Bile Salt NaDC and (b) Structure of the Secondary Aggregate of NaDC

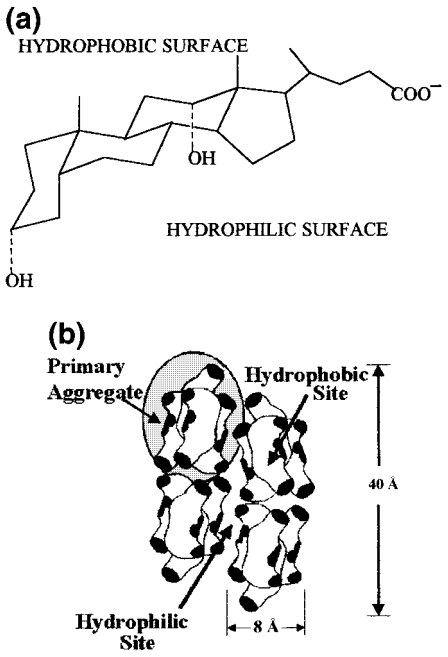

* To whom correspondence should be addressed. E-mail: pckb@mahendra.iacs.res.in. Fax: (91)-33-473-2805.

10.1021/jp0144799 CCC: $22.00
Published on Web 07/24/2002

CHART 2: (a) Structure of TNS and (b) Structure of DCM

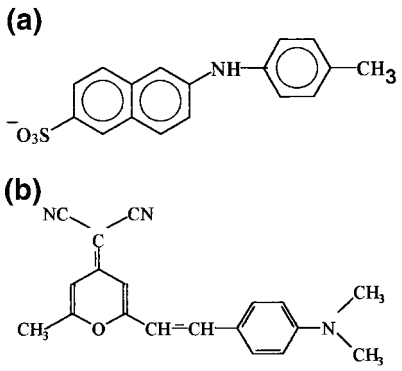

exhibits two critical micellar concentrations (CMCs) at ~10 and ~60 mM which are referred to as primary (CMC_1) and secondary (CMC_2) critical micellar concentrations, respectively.

According to Small's primary/secondary aggregation model,[15] above CMC_1 bile salts form primary aggregates with a small number of monomers (2−10). In the primary aggregate, the hydrophilic groups (hydroxyl groups and carboxylate ion, denoted by dark areas in Chart 1b) point outward. Above the second CMC (CMC_2), the primary aggregates form bigger secondary aggregates. According to recent small-angle X-ray scattering (SAXS) and small-angle neutron scattering (SANS) studies,[17−20] the structure of secondary aggregates resembles an elongated rod with a central hydrophilic core filled with water and the ions. For NaDC, the length of the rod is about 40 Å and the radius of the rod is about 8 Å.[17−20] There is a great deal of interest to understand the microenvironment of the vitally important biocavity of bile salt secondary aggregates. The polarity of the core of the bile salt aggregates has been estimated using pyrene as a fluorescent probe,[21] while Ju and Bohne[22] studied triplet quenching in bile salt aggregates.

Though there are several studies on the structure and micellar properties of bile salts, there is no report on the solvation dynamics of the water molecules in bile salt aggregates. Above CMC_2, movement of the water molecules confined in the bile salt aggregates is expected to be highly constrained. In the present work, we will demonstrate this using two fluorescent probes, 4-(dicyanomethylene)-2-methyl-(*p*-dimethylaminostyryl)-4*H*-pyran (DCM) and 2,6-*p*-toluidinonaphthalenesulfonate (TNS).

TNS (Chart 2a) is a well-known probe for many biological systems.[23] In aqueous solution, the emission quantum yield (ϕ_f) of TNS is very small (0.001) and the lifetime is also very short (60 ps). With a decrease in the polarity of the medium, ϕ_f and τ_f of TNS increase rapidly, and this is accompanied by a blue shift of the emission maximum.[23] TNS has recently been used to study solvation dynamics in many biological systems.[4] Zewail et al. detected subpicosecond components in the solvation dynamics of TNS in histone.[4a] Pierce and Boxer[4b] and Bashkin et al.,[4c] on the other hand, reported solvation dynamics of TNS on the 10 ns time scale in other proteins.

DCM (Chart 2b) has also been used to study solvation dynamics in simple solvents[24,25] and organized assemblies such as protein,[5c] micelles,[8a] and microemulsions.[7c] The main advantage of DCM as a probe for aqueous NaDC solutions is the fact that DCM is completely insoluble in water. Because of its insolubility in water, DCM resides exclusively in the interior of the bile salt, and thus, the contribution of free DCM in bulk water is completely avoided.

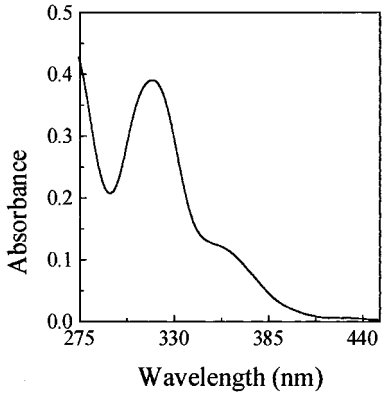

Figure 1. Steady-state absorption spectrum of TNS in 100 mM aqueous NaDC solution.

2. Experimental Section

The sodium salt of TNS (Sigma) was purified by repeated recrystallization from a methanol−water mixture. DCM (laser grade, Exciton) and NaDC (Aldrich) were used as received. The steady-state absorption and emission spectra were recorded on a JASCO 7850 spectrophotometer and a Perkin-Elmer 44B spectrofluorimeter, respectively.

Solid TNS was added to an aqueous solution of NaDC. Since DCM is insoluble in water, 20 μL of a methanolic solution of DCM was injected using a microliter syringe into 2 mL of an aqueous solution containing 100 mM NaDC. In the absence of NaDC, if a methanolic solution of DCM is injected into water, DCM is immediately precipitated. The contribution of the very small (2%) amount of methanol may be neglected, as most of it is likely to evaporate at room temperature. Further, since in methanol DCM exhibits a very fast solvation dynamics on the few picoseconds or faster time scale,[24,25] the long components detected in this work cannot be due to traces of methanol. The ϕ_f of DCM in 100 mM NaDC was calculated with respect to DCM in MeOH solution ($\phi_f = 0.44$).[24,25] The ϕ_f of TNS in aqueous NaDC solution was determined using 4-aminophthalimide in water ($\phi_f = 0.01$) as a reference.

For lifetime measurements, the sample was excited at 300 nm by the second harmonic of a rhodamine 6G dual jet dye laser with DODCI as saturable absorber (Coherent 702-1) synchronously pumped by a CW mode-locked Nd:YAG laser (Coherent Antares 76s). The emission was collected at magic angle polarization using a Hamamatsu MCP photomultiplier (2809U). The typical fwhm of the system response is about 50 ps. All measurements were done in a slightly alkaline solution of pH 8.3 ± 0.1.

3. Results

3.1. Steady-State Spectra. *3.1.1. TNS in NaDC.* Figure 1 shows the absorption spectrum of an aqueous solution of TNS containing 100 mM NaDC. It is readily seen that it is identical to that in pure water with an absorption maximum at 315 nm.

In pure water, the ϕ_f of TNS is very small (0.001) and the emission maximum is at ~465 nm.[23] On addition of NaDC to an aqueous solution of TNS, the ϕ_f of TNS increases about 110 times from 0.001 in water to 0.11 in 100 mM NaDC (Figure 2a). Along with this, the emission maximum of TNS exhibits a blue shift from 465 nm in water to 440 nm in 100 mM NaDC (Figure 2a). The 110-fold increase in ϕ_f and the significant blue shift of the emission maximum of TNS relative to water suggest that, inside the bile salt aggregate, TNS experiences an environment of polarity much less than that in bulk water.

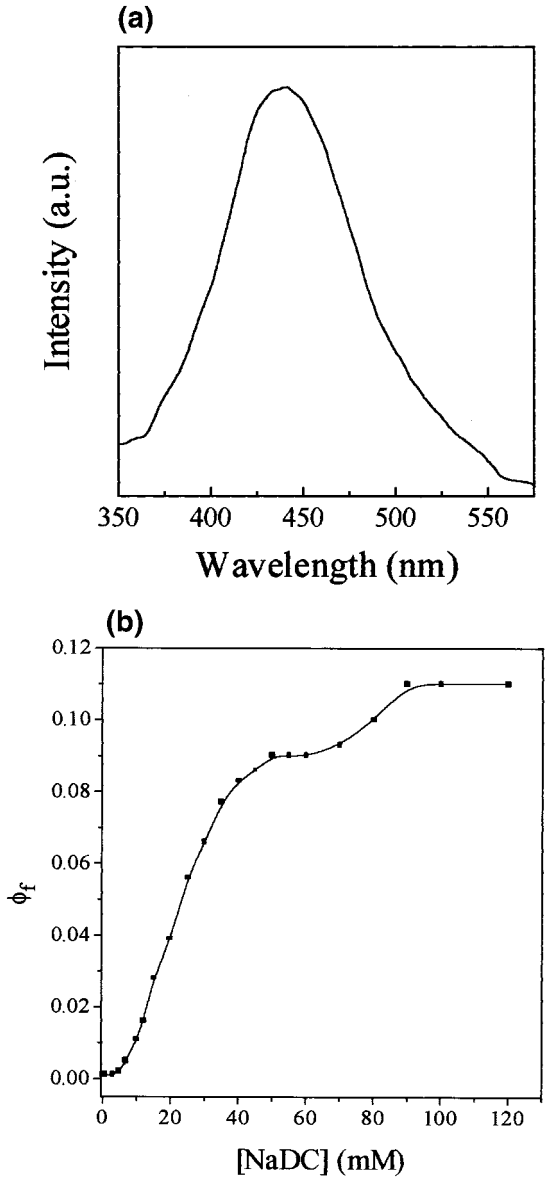

Figure 2. (a) Steady-state emission spectrum of TNS in 100 mM aqueous NaDC solution. (b) Variation of the ϕ_f of TNS with increasing concentrations of NaDC.

TABLE 1: Variation of the ϕ_f of TNS with the Concentration of NaDC

[NaDC] (mM)	ϕ_f	[NaDC] (mM)	ϕ_f	[NaDC] (mM)	ϕ_f
0	0.001	15	0.028	60	0.090
3	0.001	20	0.039	70	0.093
5	0.002	25	0.056	80	0.100
7	0.005	40	0.083	90	0.110
10	0.011	45	0.086	120	0.110
12	0.016	50	0.090		

The plot of ϕ_f against NaDC concentration shows two sharp breaks at around 7 mM and at around 60 mM (Figure 2b). This clearly suggests that the CMC_1 of aqueous NaDC is at 7 mM and the CMC_2 is at 60 mM. These values are close to the values reported by previous workers.[15,17−22] Figure 2b and Table 1 show that ϕ_f saturates above a NaDC concentration of 90 mM. As a result, the time-resolved studies are carried out in 100 mM aqueous NaDC solution.

3.1.2. DCM in NaDC. In a nonpolar medium such as *n*-heptane, DCM exhibits an absorption maximum around 450 nm and a very weak emission band with a maximum at 530 nm.[7c] When a 20 μL methanolic solution of DCM is injected into 2 mL of a 100 mM aqueous solution of NaDC, the DCM molecules bind to NaDC due to the hydrophobic interaction. The DCM molecules bound to NaDC exhibit a marked red shift of absorption and excitation maximum to 480 nm and a strong emission band with a maximum at 595 nm and quantum yield of 0.58 (Figure 3). Since DCM is insoluble in water, the steady-state spectral properties of DCM bound to NaDC could not be compared with those of DCM in water. With an increase in solvent polarity, the emission maximum of DCM displays a red shift from 530 nm in *n*-heptane to 620 nm in methanol.[24,25] It is evident that the observed emission maximum of DCM bound to NaDC is similar to that in highly polar solvents.[24,25]

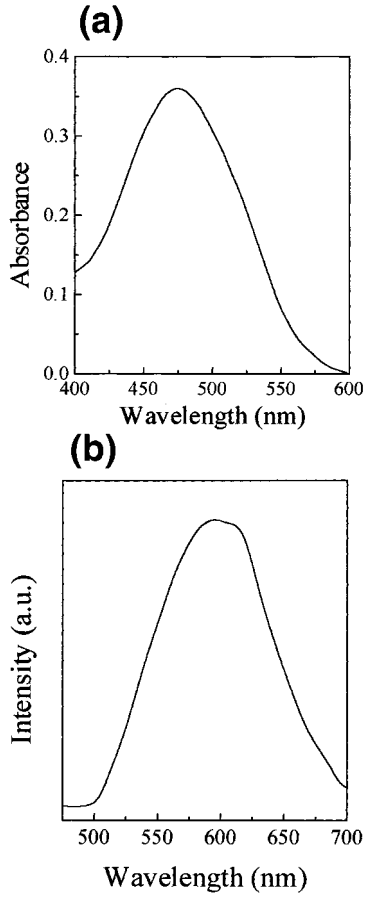

Figure 3. (a) Steady-state absorption spectrum of DCM in 100 mM aqueous NaDC solution. (b) Steady-state emission spectrum of DCM in 100 mM aqueous NaDC solution.

3.2. Time-Resolved Studies. *3.2.1. TNS in 100 mM NaDC.* In pure water, the lifetime of TNS is very short (60 ps) and the fluorescence decay does not show any wavelength dependence. However, fluorescence decays of TNS bound to bile salt aggregate exhibit substantial wavelength dependence. In a primary aggregate of NaDC, i.e., at a concentration above CMC_1 but below CMC_2, the emission decays of TNS exhibit a very long decay time of 5−6 ns and the decay is preceded by a rise. The rise component is 1450 ps at 480 nm and 590 ps at 550 nm. While the rise indicates solvation dynamics occurring in this system, the maxima of the time-resolved emission spectra (TRES) do not converge. The longer rise time at shorter emission wavelengths and the lack of convergence arise most probably from multiple environments in primary aggregates of NaDC.

In the secondary aggregate of NaDC (i.e., above CMC_2), the wavelength variation of the rise time of TNS was found to be

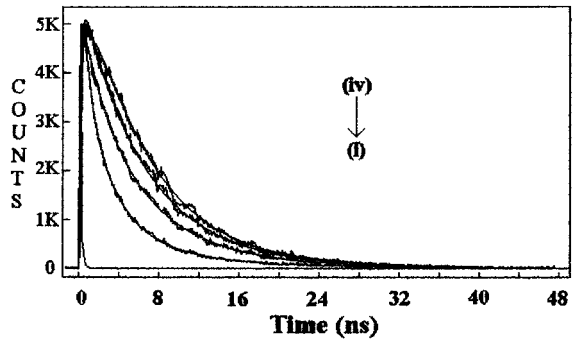

Figure 4. Fluorescence decays of TNS in 100 mM aqueous NaDC solution at (i) 390 nm, (ii) 420 nm, (iii) 440 nm, and (iii) 550 nm.

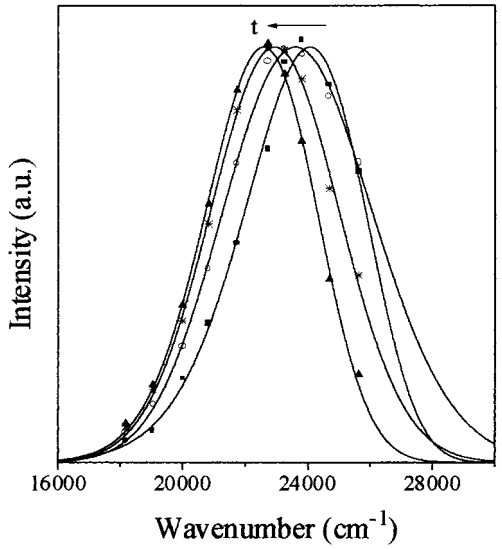

Figure 5. Time-resolved emission spectra of TNS in 100 mM aqueous NaDC solution at 25 ps (■), 300 ps (○), 2000 ps (*), and 17000 ps (▲).

quite regular and the maxima of the time-resolved emission spectra converge nicely. This indicates when TNS resides in the central water-filled core of the secondary aggregate it experiences an environment of more or less uniform properties. At the blue end of the emission spectrum (e.g., at 390 nm), the fluorescence decay of TNS in 100 mM NaDC is triexponential with three decay components of 340 ps (37%), 2.35 ns (47%), and 6.8 ns (16%) (Figure 4). However, at the red end (e.g., at 550 nm), the bile-salt-bound TNS exhibits a fluorescence decay component of 6.28 ns and a distinct growth component of 1.5 ns (Figure 4). Such a wavelength dependence clearly indicates that TNS molecules undergo solvation dynamics. Following the procedure described by Maroncelli and Fleming,[2c] the TRES (Figure 5) of TNS in 100 mM NaDC have been constructed using the parameters of the best fit to the fluorescence decays and the steady-state emission intensities. The TRES clearly show a time-dependent Stokes shift of the emission of TNS in 100 mM NaDC solution (Figure 5). The solvation dynamics is described by the decay of the response function $C(t)$, which is defined as

$$C(t) = \frac{\nu(t) - \nu(\infty)}{\nu(0) - \nu(\infty)}$$

where $\nu(0)$, $\nu(t)$, and $\nu(\infty)$ denote the observed emission energies (frequencies) at times zero, t, and infinity. The decay of $C(t)$ was fitted to a triexponential decay (Figure 6).[26] The decay parameters of $C(t)$ of TNS in 100 mM NaDC are summarized

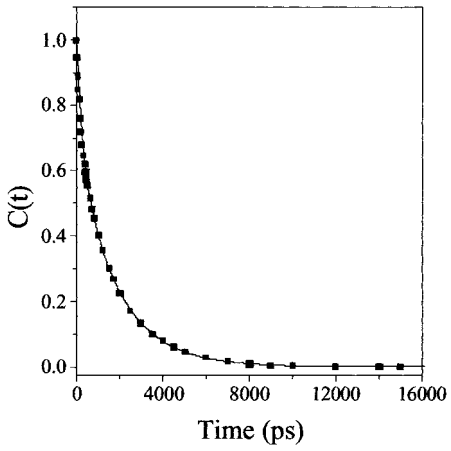

Figure 6. Decay of the response function $C(t)$ of TNS in an aqueous solution containing 100 mM NaDC. The points denote the actual values of $C(t)$, and the solid line denotes the best fit to a triexponential decay.

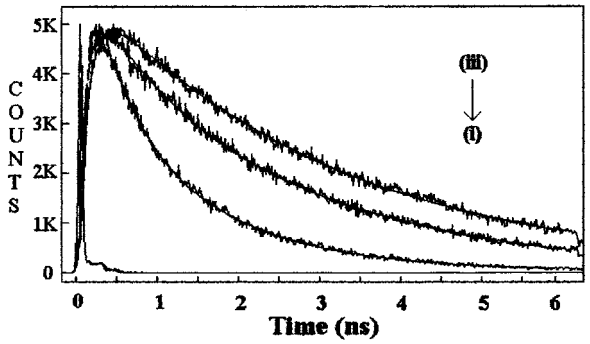

Figure 7. Fluorescence decays of DCM in 100 mM aqueous NaDC solution at (i) 520 nm, (ii) 600 nm, and (iii) 700 nm.

TABLE 2: Decay Parameters of $C(t)$ for DCM and TNS in 100 mM NaDC

probe	$\Delta\nu$ (cm^{-1})	a_1	τ_1 (ps)	a_2	τ_2 (ps)	a_3	τ_3 (ns)
TNS	1570	0.17	95	0.16	380	0.67	1.90
DCM	1600	0.19	110	0.17	700	0.64	2.75

in Table 2. In this case, the decay of $C(t)$ is found to be triexponential with components 95 ps (17%), 380 ps (16%), and 1.9 ns (67%), with the average solvation time ($\langle\tau_s\rangle = \sum a_i\tau_i$) being 1.3 ± 0.2 ns. The total Stokes shift is observed to be 1570 cm^{-1}.

3.2.2. DCM in 100 mM NaDC. The fluorescence decays of DCM bound to 100 mM NaDC are also found to be markedly dependent on the emission wavelength (Figure 7). At the blue end of the emission spectrum, only a fast decay is observed, while at the red end, the decay is preceded by a distinct rise (Figure 7). Such a wavelength dependence is a clear signature of solvation dynamics inside the bile salt aggregate. From the parameters of the best fit to the emission decays and using the steady-state emission intensities, TRES (Figure 8) of DCM in 100 mM NaDC have been constructed. The decay of $C(t)$ for DCM bound to NaDC is shown in Figure 9. The decay parameters of $C(t)$ are summarized in Table 2. The total Stokes shift, $\Delta\nu = \nu(0) - \nu(\infty)$, of DCM in NaDC is found to be 1600 cm^{-1}. The decay of $C(t)$ is found to be triexponential with components of 110 ps (19%), 700 ps (17%), and 2.75 ns (64%).[26] The average solvation time is found to be 1.9 ± 0.2 ns.

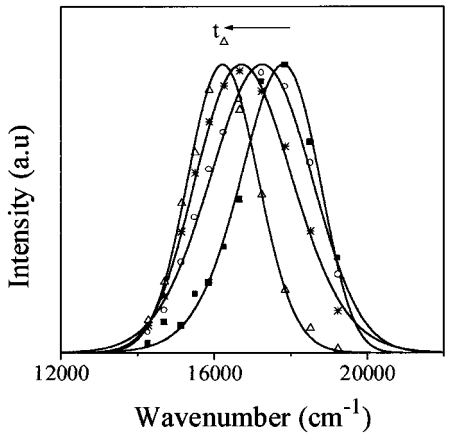

Figure 8. Time-resolved emission spectra of DCM in 100 mM aqueous NaDC solution at 0 ps (■), 400 ps (○), 2000 ps (*), and 10000 ps (△).

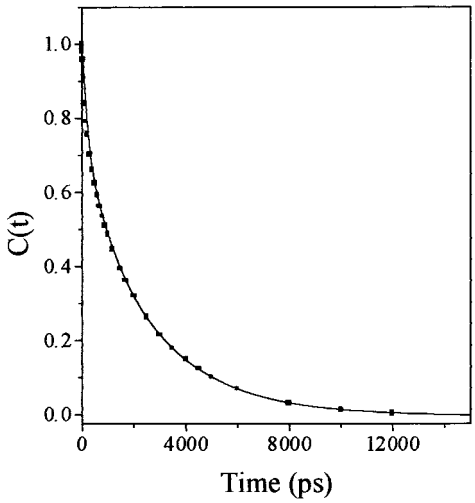

Figure 9. Decay of the response function $C(t)$ of DCM in an aqueous solution containing 100 mM NaDC. The points denote the actual values of $C(t)$, and the solid line denotes the best fit to a triexponential decay.

4. Discussion

The marked difference of the emission properties of TNS inside a bile salt aggregate from those in bulk water suggests that the probe is located inside the bile salt aggregate. In aqueous NaDC solution, DCM molecules do not stay in bulk water because of their insolubility in water. Thus, the DCM molecules stay inside the bile salt aggregate and report the properties of its interior.

It is evident that the emission properties of TNS are a sensitive indicator to follow the micellization of NaDC. The sharp increase in the ϕ_f and emission energy (i.e., blue shift) of TNS in the presence of NaDC, relative to water, indicates TNS occupies a highly nonpolar environment in the interior of NaDC micelles. Since TNS is insoluble in a hydrocarbon, it definitely stays in a hydrophilic region within the aggregates.

The steady-state absorption and emission maxima of DCM-bound NaDC indicate an environment less polar than methanol but much more polar than *n*-heptane. Thus, the DCM molecule resides in a hydrophilic region of NaDC.

Even if we conclude that the probes remain in a hydrophilic region within the bile salt aggregate, there is still some ambiguity about whether the probes stay on the external surface or in the central hydrophilic core. Also there is a possibility that within its excited-state lifetime the probe molecule may undergo an excursion from the central internal core to the external surface. However, if the probes stayed in the external surface of the secondary aggregate, they would not exhibit a sharp change of steady-state intensity and temporal characteristics of the emission as displayed by TNS above the CMC_2 of NaDC. This suggests that above the CMC_2 of NaDC, the probes are located in the central region and that the observed slow solvation dynamics reported by TNS and DCM is most probably due to the water molecules and/or the counterions trapped in the central region of the aggregates.

The most striking finding of this work is the remarkably slow solvation dynamics for both the probes in the bile salt aggregate. The solvation dynamics of DCM bound to 100 mM NaDC is found to be triexponential with components of 110 ps (19%), 700 ps (17%), and 2.75 ns (64%) having an average solvation time of 1.9 ± 0.2 ns. The solvation dynamics of TNS in 100 mM NaDC solution is also described by three components, 95 ps (17%), 380 ps (16%), and 1.9 ns (67%), with an average solvation time of 1.3 ± 0.2 ns. The small difference in the solvation times inside the bile salt aggregate reported by the two probes indicates that the solvation dynamics is reasonably independent of the probe.

Several factors may contribute to the observed markedly slow solvation dynamics inside the bile salt aggregate. First, inside the bile salt aggregate, a major portion of the trapped water molecules remain bound to the hydroxyl group of the bile salt by hydrogen bonds and to the carboxylate and sodium ions by electrostatic forces. Through these interactions, the motion of the trapped water molecules becomes coupled with the motion of the bile salt. Since the motion of the bulky bile salt is very slow, the motion of the bound water molecules becomes very slow. This results in the dramatically slow component of solvation dynamics. Nandi-Bagchi[1c] earlier used such a model to explain the slow dielectric relaxation in aqueous solution of protein and attributed the slow dynamics to an equilibrium between "bound" and "free" water molecules. Second, the slow dynamics may arise from the slow movement of counterions (Na^+) within the central core of bile salt aggregates. Huppert et al.[27] earlier reported slow solvation dynamics due to ions in molten salts. If the self-diffusion coefficient of sodium ions is 10^{-5} cm^2/s and if during solvation the sodium ion moves about 4 Å, this may lead to a time constant of 160 ps.[28] This is close to the fastest component of solvation dynamics detected in our work.

It will obviously be interesting to carry out computer simulations on the motion of water molecules inside bile salt aggregates. Such simulations have recently been carried out for water molecules bound to a micellar surface,[14a] at liquid−liquid interfaces,[14b] and in the water pool of microemulsions.[14c] These simulations reveal a universally slow component of solvation at these interfaces which is much slower than that in the corresponding liquid, in the bulk. In the most recent simulation of solvation dynamics at the surface of a micelle, Balasubramanian and Bagchi[14a] analyzed the relative contribution of various interactions of the probe (Cs^+ ion) with water and micellar headgroups. If the decay of the solvent correlation function simulated by them is fitted to a triexponential, the longest component is found to be 30 ps. Though this component is much longer than the solvation dynamics in bulk water (∼1 ps), it is much faster than the slow 100−1000 ps component detected in this work as well as in other works in many other organized assemblies.[1a,b]

In summary, the observed slow solvation dynamics is due to the slow relative motions of the polar entities (mainly trapped water molecules, Na^+ ion, and polar groups of the bile salt)

with respect to the excited fluorescent probes (TNS and DCM) inside the core of the bile salt aggregate.

5. Conclusion

This work demonstrates that TNS reliably reports the two CMCs of NaDC. From the reported structure of a bile salt aggregate,[15,17−20] it is inferred that the probes are located at the central region of the aggregate in the vicinity of trapped water and ions. It is observed that the water molecules confined in the central region of the bile salt aggregate are considerably constrained and exhibit a solvation dynamics substantially slower than that of bulk water. The observed average solvation times, 1.9 ± 0.2 ns for DCM and 1.3 ± 0.2 ns for TNS, are quite close. Thus, the solvation time is not strongly dependent on the probes. The slow dynamics of water inside the bile salt aggregate is attributed to the partial immobilization of the water molecules through attachment to the hydroxyl groups of the bile salt by hydrogen bonds and to the ions by electrostatic forces and to the dynamics of the counterions.

Acknowledgment. Thanks are due to the Council of Scientific and Industrial Research (CSIR) for generous research grants. S.S. and P.D. thank the CSIR for research fellowships.

References and Notes

(1) (a) Bhattacharyya, K.; Bagchi, B. *J. Phys. Chem. A* **2000**, *104*, 10603. (b) Nandi, N.; Bhattacharyya, K.; Bagchi, B. *Chem. Rev.* **2000**, *100*, 2013. (c) Nandi, N.; Bagchi, B. *J. Phys. Chem. B* **1997,** *101*, 10954.

(2) (a) Jarzeba, W.; Walker, G. C.; Johnson, A. E.; Kahlow, M. A.; Barbara, P. F. *J. Phys. Chem.* **1988**, *92*, 7039. (b) Jimenez, R.; Fleming, G. R.; Kumar, P. V.; Maroncelli, M. *Nature* **1994**, *369*, 471. (c) Maroncelli, M.; Fleming, G. R. *J. Chem. Phys*. **1987**, *86*, 6221. (d) Fee, R. S.; Maroncelli, M. *Chem. Phys*. **1994**, *183*, 235. (e) Silva, C.; Walhout, P. K.; Yokoyama, K.; Barbara, P. F. *Phys. Rev. Lett.* **1998**, *80*, 1086.

(3) (a) Vajda, S.; Jimenez, R.; Rosenthal, S. J.; Fidler, V.; Fleming, G. R.; Castner, E. W., Jr. *J. Chem. Soc., Faraday Trans.* **1995**, *91*, 867. (b) Nandi, N.; Bagchi, B. *J. Phys. Chem.* **1996**, *100*, 13914.

(4) (a) Zhong, D.; Pal, S. K.; Zewail, A. H. *Chemphyschem* **2001**, *2*, 219. (b) Pierce, D. W.; Boxer, S. G. *J. Phys. Chem.* **1992**, *96*, 5560. (c) Bashkin, J. S.; Mcledon, G.; Mukamel, S.; Marohn, J. *J. Phys. Chem.* **1990**, *94*, 4757.

(5) (a) Jordandies, X. J.; Lang, M. J.; Song, X.; Fleming, G. R. *J. Phys. Chem. B* **1999**, *103*, 7995. (b) Changenet-Barret, P.; Gooding, E. F.; Degrado, W. P.; Hochstrasser, R. M. *J. Phys. Chem. B* **2000**, *104*, 9322. (c) Pal, S. K.; Mandal, D.; Sukul, D.; Sen, S.; Bhattacharyya, K. *J. Phys. Chem. B* **2001**, *105*, 1438.

(6) Brauns, E. B.; Madaras, M. L.; Coleman, R. S.; Murphy, C. J.; Berg, M. A. *J. Am. Chem. Soc*. **1999**, *121*, 11644.

(7) (a) Sarkar, N.; Datta, A.; Das, S.; Bhattacharyya, K. *J. Phys. Chem.* **1996**, *100*, 10523. (b) Lundgren, L. S.; Heitz, M. P.; Bright, F. V. *Anal. Chem.* **1995**, *67*, 3775. (c) Pal, S. K.; Mandal, D.; Sukul, D.; Bhattacharyya, K. *Chem. Phys. Lett*. **1999**, *312*, 178. (d) Willard, D. M.; Riter, R. E.; Levinger, N. E. *J. Am. Chem. Soc*. **1998**, *120*, 4151. (e) Riter, R. E.; Undiks, E. P.; Levinger, N. E. *J. Phys. Chem. B* **1998**, *102*, 2705.

(8) (a) Pal, S. K.; Sukul, D.; Mandal, D.; Bhattacharyya, K. *Chem. Phys. Lett.* **2000**, *327*, 91. (b) Sarkar, N.; Datta, A.; Das, S.; Bhattacharyya, K. *J. Phys. Chem*. **1996**, *100*, 15483.

(9) (a) Datta, A.; Pal, S. K.; Mandal, D.; Bhattacharyya, K. *J. Phys. Chem. B* **1998**, *102*, 6114. (b) Pal, S. K.; Sukul, D.; Mandal, D.; Bhattacharyya, K. *J. Phys. Chem. B* **2000**, *104*, 4529.

(10) (a) Pal, S. K.; Sukul, D.; Mandal, D.; Sen, S.; Bhattacharyya, K. *J. Phys. Chem. B* **2000**, *104*, 3613. (b) Jordan, J. D.; Dunbar, R. A.; Bright, F. V. *Anal. Chem.* **1995**, *67*, 2436.

(11) (a) Zimdars, D.; Eisenthal, K. B. *J. Phys. Chem. A* **1999**, *102*, 10567. (b) Benderskii, A. V.; Eisenthal, K. B. *J. Phys. Chem. B* **2000**, *104*, 11723.

(12) (a) Riter, R. E.; Undiks, E. P.; Kimmel, J. R.; Pant, D. D.; Levinger, N. E. *J. Phys. Chem. B* **1998**, *102*, 7931. (b) Shirota, H.; Horie, K. *J. Phys. Chem. B* **1999**, *103*, 1437.

(13) Sen, S.; Sukul, D.; Dutta, P.; Bhattacharyya, K. *J. Phys. Chem. A* **2001**, *105*, 10635.

(14) (a) Balasubramanian, S.; Bagchi, B. *J. Phys. Chem. B* **2001**, *105*, 12529. (b) Michael, D.; Benjamin, I. *J. Chem. Phys.* **2001**, *114*, 2817. (c) Faeder, J.; Ladanyi, B. M. *J. Phys. Chem. B* **2000**, *104*, 1033. (d) Senapathy, S.; Chandra, S. *J. Chem. Phys.* **1999**, *111*, 207.

(15) (a) Small, D. M. *The Bile Acid*; Plenum: New York, 1971; Vol. 1, p 302. (b) O'connor, C. J.; Wallace, R. G. *Adv. Colloid Interface Sci.* **1985**, *22*, 1. (c) Borgtstorm, B.; Barrowman, J. A.; Lindstorm, M. In *Sterols and bile acid*; Danielsson, H., Sjoval, J., Eds.; Elsevier: Amsterdam, 1985.

(16) (a) Berr, S. *J. Phys. Chem*. **1987**, *91*, 4760. (b) Berr, S.; Coleman, M. L.; Jones, R. R. M.; Johnson, J. S., Jr. *J. Phys. Chem.* **1986**, *90*, 6492.

(17) Esposito, G.; Giglio, E.; Pavel, N. V.; Zanobi, A. *J. Phys. Chem.* **1987**, *91*, 356.

(18) Lopez, F.; Samseth, J.; Mortensen, K.; Rosenqvist, E.; Rouch, J. *Langmuir* **1996**, *12*, 6188.

(19) Hjelm, R. P.; Schteingert, C. D.; Hofman, A. F.; Thiagrajan, P. *J. Phys. Chem. B* **2000**, *104*, 197.

(20) Santhanlakshmi, J.; Shantha Lakshmi, G.; Aswal, V. K.; Goyal. P. S. *Proc. Indian Acad. Sci., Chem. Sci*. **2001**, *113*, 55.

(21) Gouin, S.; Zhu, X. X. *Langmuir* **1998**, *14*, 4025.

(22) Ju, C.; Bohne, C. *J. Phys. Chem.* **1996**, *100*, 3847.

(23) (a) McClure, W. O.; Edelman, L. M. *Biochemistry* **1966**, *5*, 1908. (b) Macgregor, R. B.; Weber, G. *Nature* **1986**, *319*, 70. (c) Chang, L.; Cheung, H. C. *Chem. Phys. Lett.* **1990**, *173*, 343. (d) Das, K.; Sarkar, N.; Nath, D.; Bhattacharyya, K. *Spectrochim. Acta, Part A* **1992**, *48*, 1701.

(24) (a) Gustavsson, T.; Baldacchino, G.; Mialocq, J.-C.; Pommeret, S. *Chem. Phys. Lett*. **1995**, *236*, 587. (b) van der Meulen, P.; Zhang, H.; Jonkman, M.; Glasbeek, M. *J. Phys. Chem*. **1996**, *100*, 5367. (c) Zhang, H.; Jonkman, A. M.; van der Meulen, P.; Glasbeek, M. *Chem. Phys. Lett*. **1994**, *224*, 551. (d) Jonkman, M.; van der Meulen, P.; Zhang, H.; Glasbeek, M. *Chem. Phys. Lett*. **1996**, *256*, 21.

(25) (a) Easter, D. C.; Baronavski, A. P. *Chem. Phys. Lett*. **1993**, *201*, 153. (b) Mayer, M.; Mialocq, J.-C. *Opt, Commun.* **1987**, *64*, 264. (c) Hsing-Kang, Z.; Ren-Lan, M.; Er-pin, N.; Chu, G. *J. Photochem*. **1985**, *29*, 397. (d) Retting, W.; Majenz, W. *Chem. Phys. Lett*. **1989**, *154*, 335. (e) Gilabert, E.; Lapouyade, R.; Rulliere, C. *Chem. Phys. Lett*. **1988**, *145*, 262.

(26) We have also fitted the decay of $C(t)$ to a sum of stretched exponentials, $A \exp(-t/\tau_1)^{\beta} + B \exp(-t/\tau_2)^{\beta}$. For both DCM and TNS, the stretch parameter, β, is 0.9 ± 0.02. For TNS, $\tau_1 = 130 \pm 20$ ps ($A = 0.23$) and $\tau_2 = 1600 \pm 50$ ps ($A = 0.77$). For DCM, $\tau_1 = 220 \pm 20$ ps ($A = 0.22$) and $\tau_2 = 2250 \pm 50$ ps ($A = 0.78$).

(27) Bart, E.; Meltsin, A.; Huppert, D. *J. Phys. Chem.* **1994**, *98*, 10821.

(28) We are grateful to a referee for pointing this out.